CLM-P709

CLM-P709

UKAEA

Preprint

COMMENTS ON THE STABILITY OF THE RSF 3-D MHD PLASMA SIMULATION ALGORITHM

J. W. EASTWOOD
K. I. HOPCRAFT

CULHAM LABORATORY
Abingdon Oxfordshire

1983

CLM-P 709

COMMENTS ON THE STABILITY OF THE RSF 3-D MHD PLASMA SIMULATION ALGORITHM

J.W.Eastwood and K.I.Hopcraft*

Culham Laboratory,Abingdon,Oxon,OX14 3DB,UK
(EURATOM/UKAEA Fusion Association)

ABSTRACT

A linear stability analysis of the RSF, algorithm, as published in the Journal of Computational Physics [1] is presented. It is shown that the algorithm has weak stability properties which are likely to lead to nonphysical effects dominating computational results.

* Imperial College,London

(Paper submitted for publication in Journal of Computational Physics)

(August 1983)

1. INTRODUCTION

RSF [1] is a spectral code which follows the time evolution of the Reduced MHD equations [2]. Its numerical results have been central to much development of theory of non-linear tearing modes and disruptions in Tokamaks ([2,3] and references therein). RSF has shown quantitatively different behaviour of plasma variables as magnetic Reynolds numbers are raised to values ($S \sim 10^6$) which are beyond the capabilities of existing finite difference codes.

The purpose of this note is to indicate that in reference [1]

(i) the algorithm becomes unconditionally unstable at large S

(ii) the stability criterion given is necessary but not sufficient i.e. timesteps chosen using the criterion may give numerical instability

(iii) the algorithm is unconditionally unstable to flows perpendicular to the magnetic field.

A stability diagram showing the range of stable operating parameters in RSF is given.

The results presented here refer to the *published* algorithm. The algorithm implemented in the RSF program which was used to study tearing mode activity [2,3] differs from the published one [6]. We present a detailed analysis of that algorithm in a subsequent paper [5].

2. MODEL EQUATIONS

The large aspect ratio limit orders toroidal curvature out of the equations. Consequently, the reduced equations may be written in polar (r, θ, z) or cartesian (x, y, z) coordinates with z corresponding to the toroidal direction as:-

$$\frac{\partial U}{\partial t} = - \underset{\sim}{v}_\perp \cdot \underset{\sim}{\nabla} U - S^2 (\hat{z} \times \underset{\sim}{\nabla}\psi \cdot \underset{\sim}{\nabla} j + \frac{\partial j}{\partial z}) \qquad (1)$$

$$\frac{\partial \psi}{\partial t} = -\underset{\sim}{v}_\perp \cdot \underset{\sim}{\nabla}\psi + \eta j - \frac{\partial \phi}{\partial z} - E_z^w \qquad (2)$$

$$\underset{\sim}{v}_\perp = \underset{\sim}{\nabla}\phi \times \hat{\underset{\sim}{z}} \qquad (3)$$

$$j = \nabla_\perp^2 \psi \qquad (4)$$

$$U = \nabla_\perp^2 \phi \qquad (5)$$

The definition of variables and operators follows [1]. With appropriate choice of z scale length, the magnetic field is related to the flux function by

$$\underset{\sim}{B} = \hat{\underset{\sim}{z}} \times \underset{\sim}{\nabla}\psi + \hat{\underset{\sim}{z}}$$

Equations (1)-(5) describe an incompressible magnetofluid where poloidal currents and toroidal magnetic field variations are negligible. Energy flows into the system through the wall Poynting flux, is stored in magnetic and bulk flow energy and flows out by ohmic dissipation. The model equations describe Alfvén waves and tearing modes.

A dispersion relation may be obtained by linearising Eqs. (1)-(5) about a uniform slab equilibrium in cartesian coordinates with $\eta = 1$, $j_o = U_o = 0$, $\underset{\sim}{B}_o$ = constant, $\underset{\sim}{v}_o$ = constant, and taking a disturbance $\sim \exp[i(\omega t - \underset{\sim}{k}.\underset{\sim}{x})]$:-

$$\omega_r^2 = \begin{cases} S^2(k.B_o)^2 - \left(\frac{k_\perp^2}{2}\right)^2 & ; \ \omega_r^2 > 0 \\ 0 & ; \ \text{otherwise} \end{cases} \tag{6}$$

$$\omega_i = \begin{cases} -\frac{k_\perp^2}{2} & ; \ \omega_r^2 > 0 \\ -\frac{k_\perp^2}{2} \pm \left[\left(\frac{k_\perp^2}{2}\right)^2 - S^2(k.B_o)^2\right]^{\frac{1}{2}} & ; \ \text{otherwise} \end{cases} \tag{7}$$

Equations (6)-(7) differ from the MHD results only in that k^2 is replaced by its projection $k_\perp^2$ on the poloidal plane. The modification of the Alfvén wave eigenfrequencies by the space-time lattice is the source of the numerical instabilities listed in Section 1.

3. DISCRETE APPROXIMATION

Equations (1)-(5) are discretised in polar coordinates (r, θ, z) in RSF by using a Galerkin method on a set of helical trial functions $\sim \exp[i(m\theta - nz)]$, second order finite differences to treat radial derivatives and two step second order accurate time discretisation to deal with time derivatives [1].

The algebraic equations to be solved in advancing the system from time t to time $t + \Delta t$ are

$$U^{t + \Delta t/2} = U^t + \frac{\Delta t}{2} S_u^t \tag{8}$$

$$\psi^{t + \Delta t/2} = \psi^t + \frac{\Delta t}{2} [S_\psi^t + \eta(j^{t + \Delta t/2} - j^t)] \tag{9}$$

$$U^{t + \Delta t} = U^t + \Delta t \, S_u^{t + \Delta t/2} \tag{10}$$

$$\psi^{t + \Delta t} = \psi^t + \Delta t \, S_\psi^{t + \Delta t/2} \tag{11}$$

where S_u and S_ψ are the right hand sides of Eqs. (1) and (2) with derivatives replaced by their fourier mode/finite difference approximations. Implicit treatment of the Ohmic dissipation in Equation (9) has a stabilizing effect which offsets partially the destabilizing influence of explicit advection terms.

4. STABILITY ANALYSIS

To investigate the linear stability properties of the discrete algebraic plasma model, we consider a uniform magnetised plasma in slab geometry. We take a mesh in the y direction and fourier modes in the x and z direction. This may be viewed as a local approximation to the cylindrical geometry, where r, θ and z map respectively to y, x and z.

Equilibria are defined by selecting U_o, $\underset{\sim}{B}_o$, j_o, $\underset{\sim}{v}_o$ ϕ, such that $S_u^o = S_\psi^o \equiv 0$. Dispersion and stability is analysed in the same manner as for the continuum case: Fourier analysing the linearised forms of Eqs. (8) - (11) and eliminating reference to the half timelevels gives an equation of the form

$$\begin{bmatrix} \tilde{U} \\ \tilde{\psi} \end{bmatrix}^{t + \Delta t} = \underset{\approx}{\Lambda}(\underset{\sim}{k}) \begin{bmatrix} \tilde{U} \\ \tilde{\psi} \end{bmatrix}^{t} \qquad (12)$$

for the perturbed variables $\tilde{U}$, $\tilde{\psi}$. The amplification matrix $\underset{\approx}{\Lambda}$ must have eigenvalues in the unit circle for stability [4, Chapter 4]. The dispersion relation for the numerical plasma model is

$$\det(\underset{\approx}{\Lambda} - \lambda \underset{\approx}{1}) = 0 \qquad (13)$$

where $\lambda = \exp[-i\omega\Delta t]$.

Solving Eq. (13) for the case where the plasma is at rest in the mesh frame of reference gives

$$\lambda = \frac{[1 - 2g^2(1 + ag) \pm 2g[a^2(g^2 + 1)^2 - 1]^{\frac{1}{2}}]}{(1 + 2ag)} \qquad (14)$$

where

$$g = S(\underset{\sim}{K}.\underset{\sim}{B}_o)\frac{\Delta t}{2} \quad ; \quad a = \frac{\kappa_\perp^2/2}{S(\underset{\sim}{K}.\underset{\sim}{B}_o)}$$

and $\underset{\sim}{K}$ and $\kappa_\perp^2$ are the fourier transforms of the discretised $\underset{\sim}{\nabla}$ and $\nabla_\perp^2$ operators, respectively.

Numerically stable timesteps are those for which $|\lambda| \leq 1$. Accurately represented wavelengths are those for which $i\omega' + (\lambda - 1)/\Delta t$ is small, where ω' is given by equations (6) and (7).

4.1 LARGE S LIMIT

In the limit $S \to \infty$, equation (14) reduces to $\lambda = 1 - 2g^2 \pm i2g$ giving

$$|\lambda| = [1 + 4g^4]^{\frac{1}{2}} > 1 \text{ for } g \neq 0$$

i.e. *the algorithm is unconditionally unstable at large S*

4.2 FINITE S, ZERO FLOW

The curve $a(g^2 + 1) = 1$ divides the g/a parameter space into regions where λ is real (evanscent roots) and λ is complex (oscillatory roots). The stability limit in the two instances becomes

$$\begin{aligned} -g^4 + 2ag^3 + g^2 - 1 &\leq 0; \ \lambda \text{ real} \\ g^3 - ag^2 - a &\leq 0; \ \lambda \text{ complex} \end{aligned} \qquad (15)$$

The published stability criterion [1] is $g \leq 1$: This criterion is satisfied by equations (15) only at the point $a = \frac{1}{2}$ i.e. *The published criterion is necessary but not sufficient for stability.*

4.3 NON-ZERO FLOW, $\underset{\sim}{K}.\underset{\sim}{B}_o = 0$

Non-zero flow does not simply Doppler shift frequencies as in the continuum case. It allows the possibility of further instabilities. Extending Eq. (14) to include uniform flow, $\underset{\sim}{v}_o$, is straightforward but tedious. For the special case $\underset{\sim}{K}.\underset{\sim}{B}_o = 0$, the vorticity (U) and flux (ψ) equations decouple, and the vorticity equation gives the stability criterion

$$1 + 4\left[(\underset{\sim}{K}.\underset{\sim}{v}_o)\frac{\Delta t}{2}\right]^4 \leq 1 \qquad (16)$$

i.e. *the scheme is unconditionally unstable to flows for wavenumbers such that* $\underset{\sim}{K}.\underset{\sim}{B}_o = 0$.

4.4 GENERAL CASE

Figure 1 summarises the region of the g-a plane for stable operation for a range of flow velocity parameters $b = (\underset{\sim}{K}.\underset{\sim}{v}_o)/S(\underset{\sim}{K}.\underset{\sim}{B}_o)$. Areas under the curves are regions of stability for given b. The curve for b = 0 corresponds to equality in expressions (15). Inspection of figure 1 reveals more stringent timestep limitations at large S (small a) and at small $\underset{\sim}{K}.\underset{\sim}{B}$ (large a), and a rapid collapse of the stability region with increasing flow velocity.

5. FINAL REMARKS

The numerical stability of RSF depends on the timestep, radial mesh spacing and the values of (m,n) allowed in the simulation. Thus, despite the weak stability properties of the algorithm, it is possible to initialise computations with RSF which are numerically stable. However, as the computations progress, it becomes increasingly likely that the evolution of $\underset{\sim}{B}$ and $\underset{\sim}{v}_\perp$ will move some of the permitted set of points in the g-a plane into the unstable regions shown on Fig. 1.

To avoid confusing numerical and physical effects in the result from RSF there are three complementary actions (i) maintain a running check on energy conservation (ii) monitor the position of the set of points in the (g-a) plane and (iii) perform convergence checks for different timesteps. In ref [1], it is reported that checks (i) and (iii) have been made. A further desirable step is to modify the algorithm to improve the stability properties.

H.R.Hicks of ORNL has kindly provided us with a copy of RSF to enable us to test experimentally the results of our analysis. We give in a separate paper [5] further analysis and computational results concerning the simulation of tearing modes. We note here that the computer code showed better stability than our initial analysis suggested; this we have traced to differences between the published algorithm and the coded algorithm. The algorithm coded in the program has the first two terms on the right hand side of Eq. (24), ref.[1] evaluated at timelevel $t + \Delta t/2$ rather than at timelevel t; this change ameliorates but does not eliminate numerical difficulties with the algorithm [5].

ACKNOWLEDGEMENT

The work reported here was stimulated by the interests of Dr. J. A. Wesson of the JET Joint Undertaking. We also extend our thanks to H. R. Hicks and his colleagues at ORNL for their helpful comments and for providing copies of the RSF program, test data and output.

REFERENCES

[1] H. R. Hicks, B. Carreras, J. A. Holmes, D. K. Lee and B.V. Waddell, J. Computational Phys., 44, 46-69 (1981)

[2] B. V. Waddell, B. Carreras, H. R. Hicks, J. A. Holmes Phys. Fluids, 22, 896-910, (1979)

[3] B. Carreras, H. R. Hicks, J. A. Holmes and B. V. Waddell Phys. Fluids, 23, 1811-1826 (1980)

[4] R. W. Hockney and J. W. Eastwood, "Computer Simulation using Particles", McGraw-Hill, N.Y. (1981)

[5] J. W. Eastwood and K. I. Hopcraft, "3-D Numerical Simulation of Tearing Modes in Tokamaks", to be submitted to J. Computational Physics. (1983).

[6] H.R.Hicks, private communication (1983).

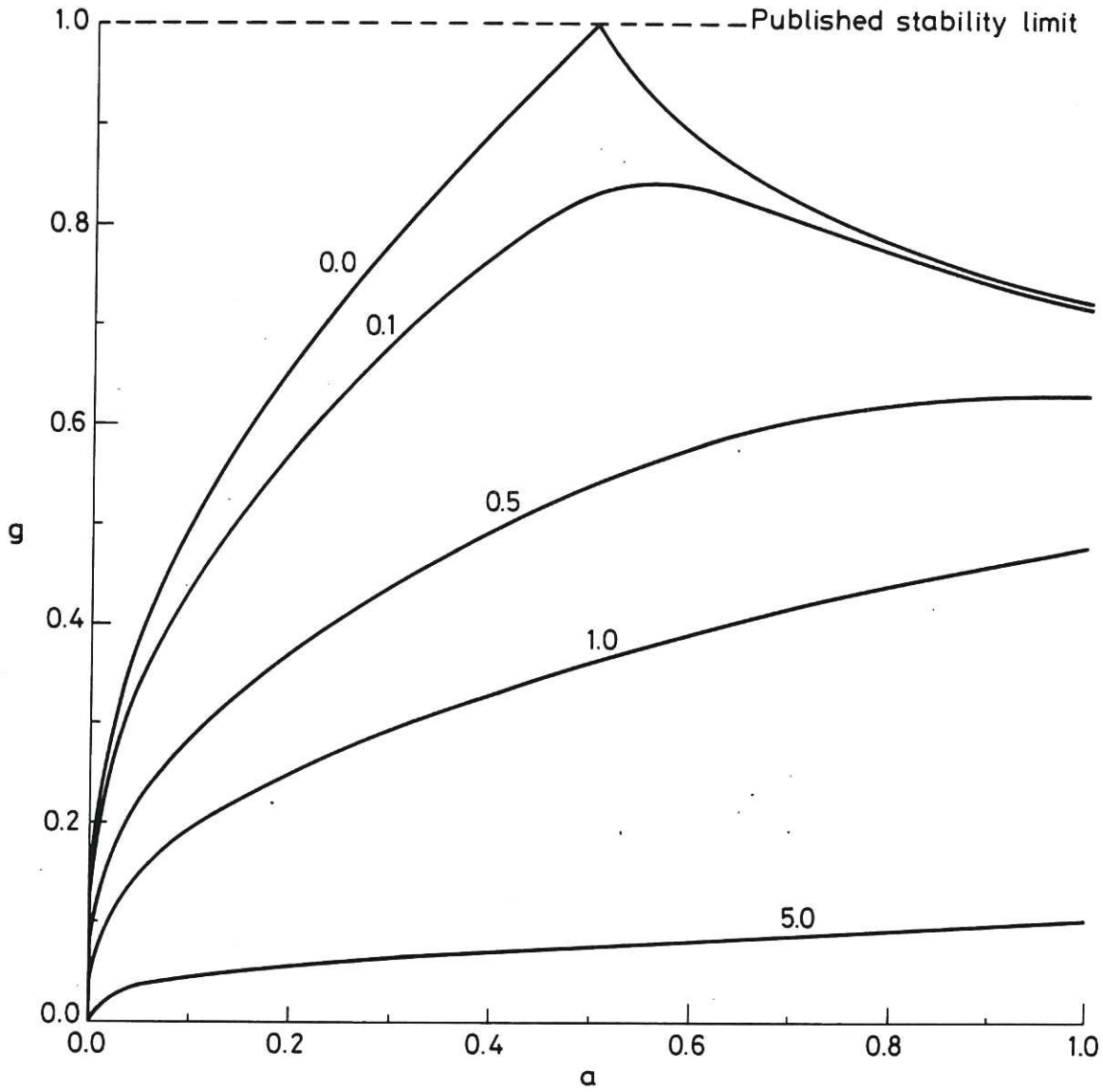

Fig. 1 Stability boundaries in the g-a plane for a range of values of b. g is the stability parameter, a is the ratio of physical wave damping to frequency and b is the ratio of the respective components of flow velocity and wave velocity parallel to wavenumber, $\underset{\sim}{K}$. Numbers labelling the curves are values of b, and regions of stability lie below the curve. The dashed line, g = 1 is the published stability criterion [1].